ТЕХНИЧЕСКИЕ НАУКИ
И ТЕХНОЛОГИИ

МАШИНА ЖАСАУ
МАШИНОСТРОЕНИЕ
MECHANICAL ENGINEERING

DOI 10.51885/1561-4212_2021_3_63
МРНТИ 55.53.13

Marek Mlynczak[1], G. Kustarev[2], N. Andrjuchov[2]
[1]Wrocław University of Science and Technology, Wroclaw, Poland
[2]Moscow Automobile and Road Construction State Technical University (MADI), Moscow, Russia
E-mail: mlymar@gmail.com
E-mail: proektdm@mail.ru
*E-mail: Nikita999-082@mail.ru**
E-mail: mlymar@gmail.com

THEORETICAL STUDIES AND CONDITIONS ANALYSIS OF THE INERTIAL SLIDER SLIPPAGE OF ASYMMETRIC PLANETARY VIBRATION EXCITER FOR SNOWPLOW

ҚАР ЖИНАҒЫШ МАШИНАҒА АРНАЛҒАН АСИММЕТРИЯЛЫҚ ПЛАНЕТАРЛЫҚ ДІРІЛ ҚОЗДЫРҒЫШТЫҢ ИНЕРЦИЯЛЫҚ ЖҮГІРТКІСІНІҢ СЫРҒУ ЖАҒДАЙЛАРЫН ТЕОРИЯЛЫҚ ЗЕРТТЕУ ЖӘНЕ ТАЛДАУ

ТЕОРЕТИЧЕСКИЕ ИССЛЕДОВАНИЯ И АНАЛИЗ УСЛОВИЙ ПРОСКАЛЬЗЫВАНИЯ ИНЕРЦИОННОГО ПОЛЗУНА АСИММЕТРИЧНОГО ПЛАНЕТАРНОГО ВИБРОВОЗБУДИТЕЛЯ ДЛЯ СНЕГОУБОРОЧНОЙ МАШИНЫ

Abstract. *Planetary vibration exciters, including their non-standard versions, are increasingly being used as pulse generators in modern utility machines. The article describes the workflow of a promising, but little-studied planetary vibration exciter with an offset (asymmetric) drive carrier axis from the driven treadmill center used to generate a directional driving force during rotation of the inertial slider. The force analysis was carried out, the reactions of the reactive forces acting on the inertial slider from the carrier and the treadmill were determined. A method has been developed for determining the critical slip angles of an inertial slider along the surface of a treadmill, which makes it possible to rationally select the design parameters of a planetary vibration exciter. A theoretical model of an asymmetric planetary vibration exciter with a pendulum anti-skid device, which adequately describes the dependence of the integral driving force on the initial parameters of the vibration exciter, is obtained. The boundary values are determined at which the slipping and skid of the slider over the treadmill surface will take place, as well as the values of the current rotation angle of the carrier, determining the boundaries of the slider skidding area, which is important for an integrated assessment of the drive torque of the vibration exciter.*

Keywords*: vibration exciter, inertial runner, carrier, eccentricity, treadmill, driving force.*

Аңдатпа. *Планетарлық діріл қоздырғыштары, оның ішінде стандартты емес өнімділігі қазіргі заманғы коммуналдық машиналарда импульстік генератор ретінде жиі қолданылады. Мақалада инерциялық жүгірткіні айналдыру кезінде бағытталған қозғаушы күш жасау үшін қолданылатын жетек жолының ортасынан жылжытылған (асимметриялық) жетек осі бар перспективалы, бірақ аз зерттелген планетарлық діріл қоздырғышының жұмыс үдісі сипатталған. Күштік талдау жүргізілді, тасымалдаушы мен жүгіру жолының инерциялық жүгірткісіне әсер ететін реактивті күштердің реакциясы анықталды. Планетарлық діріл қоздырғышының*

дизайн параметрлерін ұтымды таңдауға мүмкіндік беретін жүгіру жолының бетіндегі инерциялық жүгірткінің сыни сырғанау бұрыштарын анықтау әдісі жасалды. Маятникті сырғанауға қарсы құрылғысы бар асимметриялық планетарлық діріл қоздырғышының теориялық моделі алынды, интегралды қозғаушы күштің діріл қоздырғыштың бастапқы параметрлеріне тәуелділігін барабар сипаттайды. Жүгірткінің жүгіру жолының беті бойымен сырғуы және сырғуы болатын шекаралық мәндер, сондай-ақ драйвер жетегінің моментін жан-жақты бағалау үшін маңызды жүгірткінің сырғу аймағының шекараларын анықтайтын драйвердің ағымдағы айналу бұрышының мәндері анықталады.

Түйін сөздер: *діріл қоздырғышы, инерциялық жүгіруші, тасымалдаушы, эксцентриктілік, жүгіру жолы, қозғаушы күш.*

Аннотация. *Планетарные вибровозбудители, в том числе их нестандартные исполнения, все чаще используются в качестве генератора импульсов в современных коммунальных машинах. В статье описывается рабочий процесс перспективного, но малоизученного планетарного вибровозбудителя со смещенной (асимметричной) осью привода от центра приводной беговой дорожки, используемого для создания направленной движущей силы при вращении инерционного ползуна. Был проведен силовой анализ, определены реакции реактивных сил, действующих на инерционный ползунок со стороны носителя и беговой дорожки. Разработан метод определения критических углов скольжения инерционного ползуна по поверхности беговой дорожки, позволяющий рационально выбирать конструктивные параметры планетарного вибровозбудителя. Получена теоретическая модель асимметричного планетарного вибровозбудителя с маятниковым противоскользящим устройством, адекватно описывающая зависимость интегральной движущей силы от начальных параметров вибровозбудителя. Определяются граничные значения, при которых будет происходить скольжение и скольжение ползуна по поверхности беговой дорожки, а также значения текущего угла поворота водила, определяющие границы зоны скольжения ползуна, что важно для комплексной оценки крутящего момента привода вибровозбудителя.*

Ключевые слова: *вибровозбудитель, инерционный бегун, носитель, эксцентриситет, беговая дорожка, движущая сила.*

Introduction. During the construction of roads and other engineering structures, a significant amount of work is related to the compaction of soils and other materials, and the compaction quality directly affects the reliability and durability of structures. A progressive dynamic-type compacting tool is a vibration technique, which is represented by vibratory rollers and vibratory plates. Vibro-compaction is an effective method of compaction, both of non-cohesive materials and viscoplastic the interaction between particles, in this case, is determined only by friction forces, which are significantly reduced when the mass of the material is involved in the oscillatory process.

Nowadays, vibration machines are becoming increasingly common in construction, the main advantages of which, as compared with static ones, are: higher productivity; less metal consumption – 4-12 times; lower operating costs. In most cases, the dynamic soil compaction is better and more efficient. The working body of the vibratory roller is a metal roll of a hollow welded structure with a vibration exciter inside. Installation of the exciter directly on the frame of the roller leads to a more complex and cumbersome design, moreover, is subjected to strong vibration effects. In the designs of modern vibratory rollers, new technical solutions have appeared, aimed at improving the quality of compaction, introducing control of the material density degree from the driver workplace during the compaction process, more fully utilizing the capabilities of vibration exciters. They allow generating a driving force of directional action and reducing the number of sealing passes and sizes rollers due to the magnitude of the smoothly variable external static force, to improve the working conditions of the driver and technical cars service.

A special place among the designs of periodic power generators is occupied by planetary-type vibration exciters, as they allow obtaining more complex types of action force depend-

ence on time than a purely harmonic one. As a rule, in planetary vibration exciters, a massive slider is used, moving along the side of the body in a shape that differs from the circular one [1-4]. This allows getting a wider range of periodic effects types, but their practical use requires the solution of several applied problems. The main task is to transfer the dynamic effect on the axis of the vibration exciter and to ensure the movement of the slider through the shell without strikes and slippage. These deficiencies are eliminated by the structures of planetary exciters, in which the movement of the slider is consistent with the parameters of the shell with the help of a rigid kinematic connection. In addition, there are approaches to the design of vibration exciters, combining circular and linear vibrations and implementing more complex types of force action [5-7].

Currently, there are vibration exciters with a displaced center of rotation – asymmetric planetary vibroexciters (APV). APV can be with a round and non-circular treadmill, for example, elliptical. Both types of APV have one drawback – the inertial slider slipping on the treadmill surface, under the action of inertial forces, which, depending on the carrier rotation angle, set the inertial slider or slip, or move with the skid.

Thus, the main task of this research is to determine whether the inertial runner can move along the treadmill surface, examining vibration exciters with a round treadmill shape.

Materials and methods of research. A characteristic disadvantage of symmetrical and asymmetrical planetary vibroexciters is the inertia slider slipping along the treadmill surface under the action of inertial forces in the transient movement of the vibration exciter body. The parameters are determined by the size of the driving force and the mass of the vibration exciter, as well as the physicomechanical characteristics of the deformed area [8-11]. Slider slippage, when the optimal variant of its rolling on the treadmill fails, leads to a sharp (about ten times) increase in the carrier resistance moment and power consumption of the vibration exciter, and with a limited drive motor power – to limit the frequency or disrupt oscillations. In the most adverse conditions, it is also possible to tear the inertial slider from the surface of the treadmill. Intensive heating and abrasive wear of the inertial slider and treadmill surface are observed.

Figure 1a shows a block diagram of an asymmetric planetary vibration exciter with a powered carrier, and Figure 1b shows the calculated scheme of asymmetric planetary vibroexciter (APV) with a carrier of the leash type, where the inertial slider is represented as a material point.

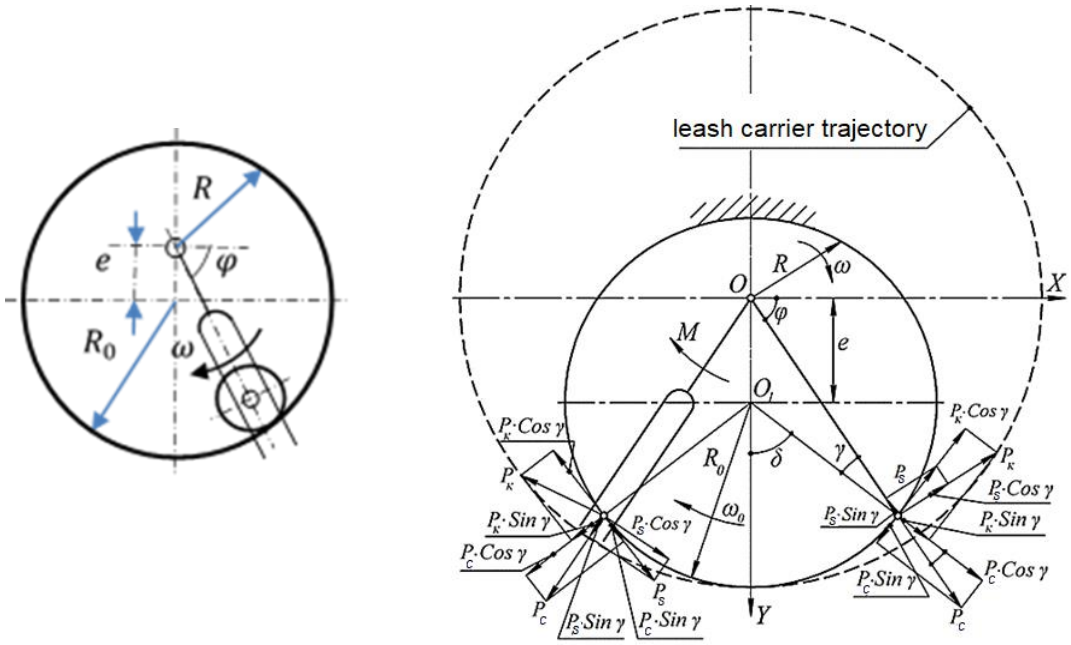

Figure 1. The design scheme of the APV with a leash type carrier

The carrier rotation axis *0* is shifted relative to the center of curvature *01* of the treadmill to the eccentricity *e* taking the radius of the treadmill *R0*, the following values are obtained from the geometric relationships by solving equations:

$$R_0 cos\delta = Rsin\varphi - e; R_0 sin\delta = Rcos\varphi; \quad (1)$$

where R – current rotation radius of the inertial slider relative to the rotation carrier axis; φ – current angle of inertia slider rotation R; δ – current rotation radius R_0 rotation of the inertial runner relative to the treadmill curvature center.

When solving equations (1) relative to the radius R, the absolute value of the current radiusis obtained

$$R = e\left[sin\varphi + \sqrt{\left(\frac{R_0}{e}\right)^2 - cos^2\varphi}\right] \quad (2)$$

Due to the eccentricity, the inertial slider not only performs an asymmetric circular motion around the center *01*, but also periodically moves along the radius of rotation with a radial velocity $dR/d\varphi$. Differentiating the equation of radius R by the magnitude of the elementary current angle of rotation $d\varphi$, the alternating radial velocity is obtained

$$\frac{dR}{d\varphi} = \frac{eR\cos\varphi}{R - \sin\varphi} = e\cos\varphi\left[1 + \frac{\sin\varphi}{\sqrt{\left(\frac{R_0}{e}\right)^2 - \cos^2\varphi}}\right] \quad (3)$$

The magnitude of the current angle δ with regard to formula (2) is determined by the trigonometric dependencies

$$cos\delta = sin\varphi\sqrt{1-\left(\frac{e}{R_0}\right)^2 cos^2\varphi} - \frac{e}{R_0}cos^2\varphi\ ;$$
$$sin\delta = cos\varphi\sqrt{1-\left(\frac{e}{R_0}\right)^2 cos^2\varphi} + \frac{e}{R_0}cos\varphi sin\varphi\ . \quad (4)$$

The angle γ between the current radii of rotation R and the curvature $R0$ is determined by the dependence $\gamma = \varphi + \delta - \pi/2$. Then $cos\gamma = sin(\varphi+\delta)$, and $sin\gamma = -cos(\varphi+\delta)$. Using expression (4), the equation is

$$cos\gamma = \sqrt{1-\left(\frac{e}{R_0}\right)^2 cos^2\varphi}\ ; \qquad sin\gamma = \frac{e}{R_0}cos\varphi$$
$$sin\delta = \cos(\varphi-\gamma)\ ; \qquad cos\delta = sin(\varphi-\gamma) \quad (5)$$

It should be noted that at the points $\varphi = \pi/2$ and $\varphi = 3\pi/2$, the $\sin\gamma$ function reverses sign, whereas the $\cos\gamma$ function remains positive over the entire range of variation of the angle φ.

In asymmetric planetary vibroexciters, the rotation carrier center is shifted relative to the treadmill curvature center by the eccentricity amount. The additional effect on the increase of driving force and the multi-frequency nature of vibrations is provided by an additional effect on the inertial slider of the Coriolis inertia forces due to the variable radius of inertial runner movement relative to the carrier rotation center of the constant angular velocity of rotation of this carrier or due to the variable angular velocity of slider movement relative to the treadmill curvature center at a constant radius path of movement [12-13]. However, this additional effect is simultaneously accompanied by an increase in the slider's slippage probability on the treadmill. The alternating radial velocity $dR/d\varphi$ of the inertial slider relative to the carrier rotation center determines the uneven effect of the Coriolis forces on the parts of the slider that are distant at different distances from the specified center. As a result, the slider acts on the entire circular trajectory of movement except for points $\varphi \pm 0.5\pi$ of Coriolis torque, which in certain parts of the trajectory determines the slider's spontaneous slippage: its slipping within the arc of the trajectory ($-0.5\ \pi < \varphi < 0{,}5\pi$) and skid in the range $0.5\pi < \varphi < 1.5\pi$. In addition, the additional torque ensures the discrepancy between the vector of the radial centrifugal force and the radius of the treadmill [14]. It is possible to an unfavorable combination of conditions for inertial slider slipping under the action of centrifugal and Coriolis forces and additional inertial forces in the transient movement of the exciter body due to the deformation of the environment.

To determine the true effectiveness of the asymmetric planetary vibroexciter and the development of constructive measures to prevent the inertial creeper from slipping, it is necessary to find the angular coordinates of the creeping sites within the circular motion path of the crawler [15-17]. The centrifugal angle of these sections increases with an increasing eccentricity of the carrier and the specific rolling radius of the inertial slider is referred to as the radius of curvature of the ring treadmill. Thus, the task of the study is reduced to the determination of the critical values of the angle φcr of the turn of the carrier, at which the inertia slider begins and ends on the treadmill. The critical angle φcr can be found from the condition $Pkas = Psc$, where $Pkas$ is the tangential force acting at the point of contact of the inertial slider with the treadmill; Psc - the grip force of the slider with the surface of the treadmill, which is determined by the product of the normal reaction of the treadmill on the slider and the coefficient of friction of the slider on the treadmill [18-20].

$$P_{kas} = m\omega^2 R\left(sin\gamma + \frac{32}{9\pi^2}\frac{r}{R}tg\gamma \right) = m\omega^2 R\left(sin\gamma + \frac{32}{9\pi^2}\frac{r}{R_0}\frac{tg\gamma}{K_e^{-1}sin\varphi + cos\gamma} \right) \quad (6)$$

where m – the mass of the inertial runner; ω – angular speed of carrier rotation; R – current radius of curvilinear motion of the slider relative to the axis of rotation of the carrier,

$$R = R_0\left(K_e^{-1} \cdot sin\varphi + cos\gamma\right);$$

R_0 – radius of curvature of the ring track; K_e – drove eccentricity coefficient, $K_e^{-1} = \frac{e}{R_0}$;

e – eccentricity of the axis of rotation of the carrier relative to the center of curvature of the treadmill; φ – current angle of rotation relative to perpendicular to eccentricity; γ – variable angle between radii R and $R0$, $\gamma = arcsin\left(K_e^{-1} \cdot cos\varphi\right)$; r – rolling radius of the inertial runner on the treadmill.

Grip strength *Psc* is determined separately for the right and left branches of the trajectory of the inertial slider [14].

For the interval ($-0{,}5\,\pi < \varphi < 0{,}5\pi$):

$$P_{sc} = \frac{m\omega^2 R \cdot f_{sc} \cdot cos\gamma}{1-(f_{sc} - f)\cdot tg\gamma} \quad (7)$$

where $f$sc – friction coefficient (sliding friction) of the inertial runner with the surface of the treadmill; f – inertial slider rolling resistance coefficient.

For the interval $0{,}5\pi < \varphi < 1{,}5\pi$:

$$Psc = \frac{m\omega^2 R \cdot f_{sc} \cdot cos\gamma}{1+ f_{sc} \cdot tg\gamma} \quad (8)$$

The difference in the values of *Psc* is determined by different conditions of slip and the progress of the slider. Since the function *tgγ* changes sign when moving from one interval to another, this difference reduces only to the fact that in the denominator the factor *(fsc - f)* for the slider mode of the slider is replaced by the factor *fsc* for the user mode. From the equality *Pkas* = *Psc*, follows for the interval *(- 0.5 π <φ <0.5π):*

$$\sin\gamma + \frac{a \cdot tg\gamma}{K_e^{-1} \cdot sin\varphi + cos\gamma} = \frac{f_{sc} \cdot cos\gamma}{1-(f_{sc} - f)\cdot tg\gamma} \quad (9)$$

and for the interval $0{,}5\pi < \varphi < 1{,}5\pi$:

$$\sin\gamma + \frac{a \cdot tg\gamma}{K_e^{-1} \cdot sin\varphi + cos\gamma} = \frac{f_{sc} \cdot cos\gamma}{1+ f_{sc} \cdot tg\gamma} \quad (10)$$

where

$$a = \frac{32}{9\pi^2}\frac{r}{R_0} = 0{,}36\frac{r}{R_0} \quad (11)$$

An analytical study of the functions obtained shows that with an increase in the ratio, with increasing radius of the slider, the magnitude of the coefficient of eccentricity drove K, corresponding to the values of the critical current angle of rotation of the carrier φcr, at which the slider slips, it will decrease. Consequently, with an increase in the ratio runner slippage proba-

bility increases. With a constant value of eccentricity e with an increase in the ratio the central angle of the creeping arc of the slider increases both in the left and in the right branch of the trajectory defined by the treadmill. On the contrary, with an increase in the friction coefficient fsc, the value of K, corresponding to the values of the critical angle φcr, will increase, i.e. the central angle of each slider creeping arc decreases, moreover, the probability of its creeping goes down.

The general solution of the obtained transcendental equations related to the angle $\varphi = \varphi cr$ is difficult since in algebraic form it leads to solving an equation of the 16th degree. More convenient is the particular solution, for example, by the method of successive approximations for finding the values of the coefficient K = according to the values of the angle φ = φcr given with a certain step for certain values of the parameters, f, and fsc. A graphic interpretation of this solution is shown in Fig. 2 for values fsc = 0.2; f = 0.02; = 0.1.

The maximum probability of inertial slider slipping corresponds to the positions of the carrier φ=0 and φ=π, i.e. when the carrier is located perpendicular to the eccentricity of its rotation axis. For this maximum probability, the slippage mode occurs at the minimum values of the K coefficient and eccentricity e. Curves determine the values of the critical angles φcr of the carrier turn, at which the slider slip begins and ends. The area between the curves and the axis of ordinates corresponds to the reliable operation of the exciter without slipping the slider when.

The shaded areas to the right of the curves (Fig. 2) mean guaranteed slider slipping on the treadmill when Psc < Pkas. To determine the central angles of each arc of the slider's slider in the left and right branches of the movement trajectory, it is necessary to find the difference of the ordinates of each shaded area of the graph corresponding to the value of the eccentricity coefficient K under consideration.

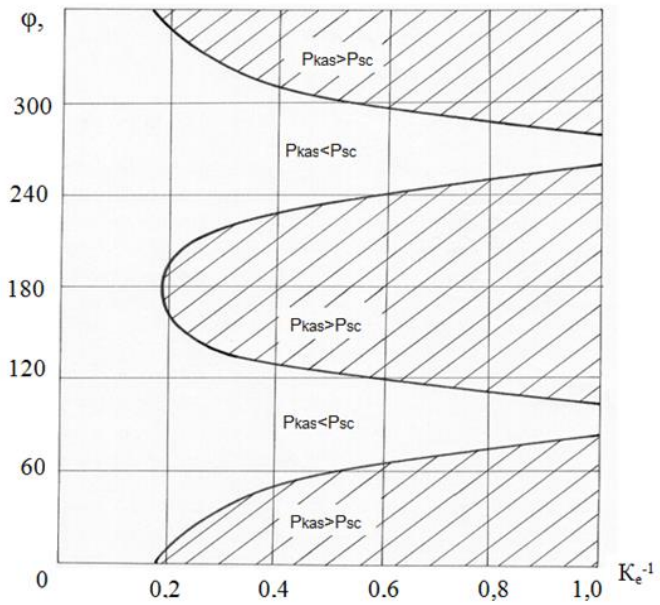

Figure 2. Dependence of the angular coordinates of slipping areas on the exciter carrier eccentricity within the circular path of the inertial slider

For example, for K-1 = 0.4, the slip of the slider will occur within the arc φ = 3000…600 or φ = φ = –600…600, and the slider skid - within the arc φ = 1200…2400, i.e. the length of the

left and right arc slider is 1200, and only within 1200 of the central angle of the movement path slider moves without slipping. With the values and the slippage probability tends to zero, i.e. the angle φcr corresponds to infinitely large values of $K_e^{-1} \to \infty$. This is explained by the fact that in the indicated positions of the carrier, the Coriolis force acting on the slider changes its sign and passes through zero, and the vector of centrifugal force coincides with the radius of rotation of the slider R relative to the axis of rotation of the carrier. Therefore, the tangential force is *Pkas min* (the minimum is determined only by the rolling resistance of the slider $PS = Pc \cdot f$), and the adhesion force is maximum $Psc = Pc \cdot fsc$, where *Pc* is the centrifugal force.

For the accepted values of the parameters fsc, f and the minimum value of the coefficient K at which the slider slips K 0,196 at points φ=0 and φ=π, and for skid at least K is slightly larger (by 0.35%) than for slider. Thus, the slider is a more dangerous critical mode of its movement compared to the skid.

The developed method for determining the critical inertial slider slip angles along the treadmill surface makes it possible to rationally select the design parameters of an asymmetric planetary vibration exciter and additional means of preventing the inertia movement slipping, which can provide a significant reduction in the energy intensity of work, increase the efficiency and reliability of the vibration exciter.

In the well-known constructions of asymmetric planetary vibration exciters, no devices are preventing the inertial sliders from slipping.

As a result of research and development, many anti-skid device designs have been developed that prevent inertial creep from slipping. The most effective is the design of a pendulum-type anti-skid device, pivotally connected by a pendulum with an inertia slider axis, the load of which has the possibility of free deflection relative to the radial arrangement (Fig. 3).

Consider the workflow of an asymmetric planetary vibration exciter with a pendulum anti-skid device, in which the additional inertial mass is pivotally mounted on the axis of the inertial runner using a pendulum and moves along a path with a variable radius exceeding the treadmill radius. The resultant centrifugal and Coriolis forces, which are applied to the load of the pendulum, are transmitted to the axis of the runner, additionally pressing it to the treadmill. Fig. 3 shows a block diagram of an asymmetric planetary vibration exciter with a pendulum anti-skid device and a flood carrier, the inertial slider of which is represented as a material point. The axis of rotation of carrier 01 is shifted relative to the center of curvature 0 of the treadmill to eccentricity *e*. The inertial slider periodically moves along the radius with a variable radial velocity.

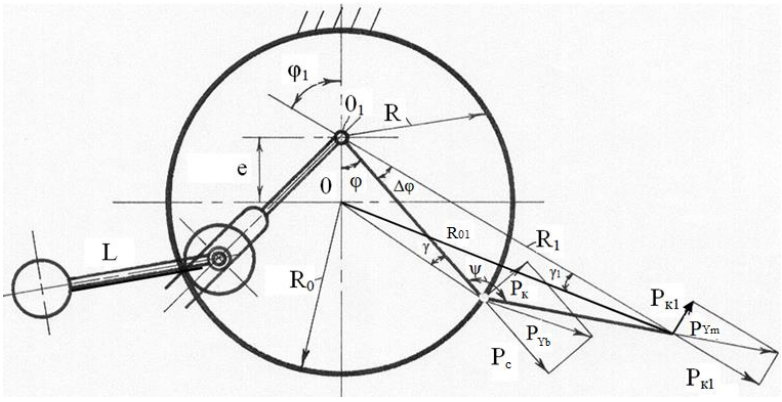

Figure 3. Design diagram of an asymmetric planetary vibration exciter with a carrier

and a pendulum anti-skid device

To analyze the dynamics of the exciter with a pendulum anti-skid device, consider the forces acting on the slider and pendulum [7, 11]. The value of the current radius of rotation of the inertial slider *R* and the formula for the inertial forces acting on the inertial slider obtained from the geometric relations.

The pendulum anti-skid device is affected by the forces:

Pc1 – centrifugal inertial force acting on the mass center of pendulum anti-skid device:

$$Pc1 = m1 \cdot \omega_1^2 \cdot R1 \tag{12}$$

where *m* where *m1* – mass of the pendulum anti-skid device; *R1* – current rolling radius of the mass center of the pendulum anti-skid device,

$$R1 = \sqrt{L^2 + R^2 - 2RL\cos\psi}\,; \tag{13}$$

Ψ – the angle between the pendulum and the carrier;

ω*1* – rotational speed of the center of mass of the pendulum,

$$\omega 1 = \omega \cdot \sqrt{\frac{R}{L}}\,; \tag{14}$$

L – ever length of the pendulum skid device.

Pк1 – Coriolis inertia force acting on the center of mass of the pendulum anti-skid device

$$Pк1 = 2\, m1 \cdot \omega_1^2 \cdot \frac{dR_1}{d\varphi_1} \tag{15}$$

where *φ1* – the current rotation angle of rotation radius of the inertial mass center of the pendulum anti-skid device.

The angle *ψ* between the pendulum and the carrier of the inertial slider cannot be determined on the basis of the known equations [7] describing the process of planetary motion. At the same time, experimental studies on a model of an asymmetric planetary vibration exciter with a stroboscopic fixation of the pendulum positions with a load for different load values and the carrier rotation frequency showed that the angle, quite uniquely depends on the specified parameters, is a deterministic factor that can be uniquely determined by the functional dependence on the initial parameters of the planetary motion. Based on the fact that, as indicated above, the analytical definition of this functional dependence causes difficulties [7], it is proposed an empirical dependence of the angle *ψ* on the initial parameter - the current angle *φ* of the exciter rotation, on the basis of which the general solution of the inertial slider equations was obtained with pendulum anti-skid device.

Angle *ψ*, equal to the mass center deviation of the pendulum from the carrier axis, when conducting experimental studies on an asymmetric planetary vibration exciter, varies within *1350<ψ<2250*, with the maximum deflection of the pendulum corresponding to the carrier position at *φ=900* and *φ=2700*, and at *φ=1800* and *φ=3600* angle *ψ=1800*. It is conventionally assumed that the deviation of the pendulum from the carrier axis in each quadrant of the treadmill depends on the angle *φ* and does not exceed the angle *(1800–ψ)=±450* when the angle values are *φ=900* and *φ=2700*. The values of the angle *ψ* sinusoidally depend on the angle *φ* and correspond to the graph shown in Fig. 4 for any angular velocity drove the exciter *ω* and eccentricity *e*. This graph is approximated by the expression:

$$\psi = 1{,}085\,(\pi - \sin\varphi) \tag{16}$$

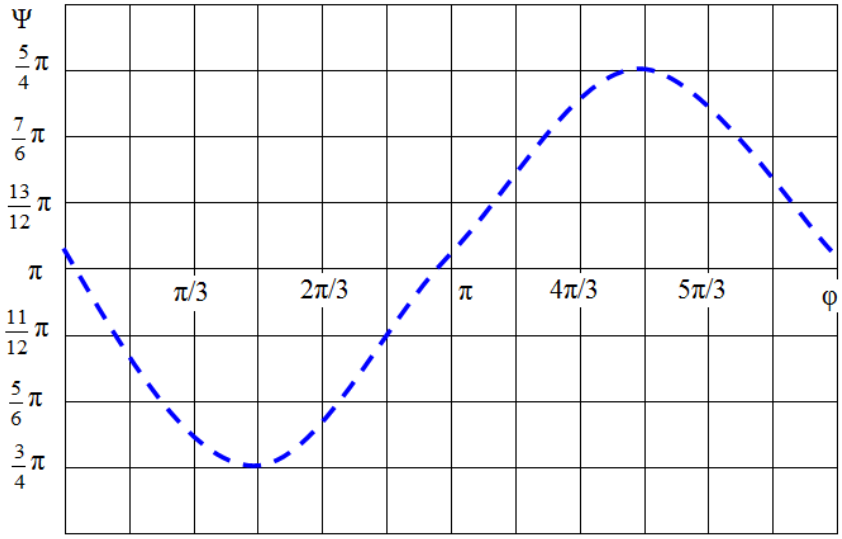

Figure 4. Dependence of the angle ψ deviation between carrier axis and pendulum axis of the from the carrier rotation angle of the exciter φ

The force acting along the radius *R1* is $Pn\varphi = Pc1$, and the additive tangential force $P^{\tau\delta}$, perpendicular to the radius *R01*, when its positive value coincides with the direction of carrier rotation when $0 < \varphi 1 < \frac{\pi}{2}$:

$$P\tau\,\delta 1 = Pc1 \cdot \sin\gamma 1 - P\kappa 1 \cdot \cos\gamma 1 \tag{17}$$

The additive tangential force $P\tau\varphi 1$, which characterizes the moment of pendulum rotation resistance

$$P\tau\varphi 1 = -P\kappa 1. \tag{18}$$

The same as *Pk*, the force *Pk1* directly depends on the function $\cos\varphi 1$ and is always directed at an angle $\frac{\pi}{2} - \varphi_1$ to the vertical axis Y of the vibration exciter in the direction of the eccentric displacement of the carrier rotation axis throughout the entire range of $\varphi 1$ values.

The projection of the full driving force on the Y axis consists of two parts:

$$PY = PYb + PYm \tag{19}$$

where *PYb* – component of the total driving force from the inertial slider.

PYm – component of the total driving force from the inertial forces of the pendulum anti-skid device.

$$P_{Yb} = P_{\tau\varphi}\sin\varphi + P_{n\varphi}\cos\varphi = -2P_c tg\gamma\sin\varphi + P_c\cos\varphi = P_c(\cos\varphi - 2tg\gamma\sin\varphi); \tag{20}$$

where

$$\gamma = arcsin\left(\frac{e}{R_0}\cdot\sin\varphi\right) \tag{21}$$

Then $$PYb = Pc\,[\cos\varphi - 2\sin\varphi \cdot tg(\arcsin\frac{e}{R_0}\cdot\sin\varphi)] \quad (22)$$

Substituting in the resulting expression the values of *Pc* and *R*, it is obtained:

$$PYb = m\omega 2\cdot[e\cdot\cos\varphi + \sqrt{R_0^2 - e^2\cdot\sin^2\varphi}\,]\cdot[\cos\varphi - 2\sin\varphi\cdot tg(\arcsin\frac{e}{R_0}\cdot\sin\varphi)] \quad (23)$$

$$P_{Ym} = P_{\tau\varphi_1}\cdot\sin\varphi_1 + P_{n\varphi_1}\cdot\cos\varphi_1 = -2P_{cm}\cdot tg\gamma_1\cdot\sin\varphi_1 + P_{cm}\cdot\cos\varphi_1 = \\ = P_{cm}(\cos\varphi_1 - 2tg\gamma_1\cdot\sin\varphi_1) \quad (24)$$

where $$\gamma_1 = \arcsin\left(\frac{e}{R_{01}}\cdot\sin\varphi_1\right); \quad (25)$$

$$\varphi 1 = \varphi + \Delta\varphi; \quad (26)$$

$$\Delta\varphi = \text{arctg}\,\frac{L\cdot\sin\psi}{R - L\cdot\cos\psi}; \quad (27)$$

$$\varphi 1 = \varphi + arctg\frac{L\cdot\sin[1{,}085(\pi - \sin\varphi)]}{R - L\cdot\cos[1{,}085(\pi - \sin\varphi]} \quad (28)$$

Consequently:

$$PYm = mM\omega 2\,\frac{R\cdot R_1}{L}\left[\cos\varphi_1 - 2\sin\varphi_1\cdot tg\left(\arcsin\left(\frac{e}{R_{01}}\cdot\sin\varphi_1\right)\right)\right] \quad (30)$$

The final expression for the driving force acting along the Y axis after transformations:

$$PY = \quad m\omega 2R0\left\{\left[\frac{e}{R_0}\cdot\cos\varphi + \sqrt{1 - \frac{e^2}{R_0^2}\cdot\sin^2\varphi}\right]\cdot\left[\cos\varphi - 2\sin\varphi\cdot tg\left(\arcsin(\frac{e}{R_0}\cdot\sin\varphi)\right)\right] + \right.$$
$$\left. + \frac{K_M\cdot\left(\frac{e}{R_0}\cdot\cos\varphi + \sqrt{1 - \frac{e^2}{R_0^2}\cdot\sin^2\varphi}\right)\cdot R_1}{L}\cdot\left[\cos\varphi_1 - 2\sin\varphi_1\cdot tg\left(\arcsin(\frac{e}{R_{01}}\cdot\sin\varphi_1)\right)\right]\right\} \quad (31)$$

where *R01* – текущий радиус вращения центра масс маятника относительно центра кривизны беговой дорожки, the current rotation radius of the pendulum mass center relative to the treadmill curvature center

$$R_{01} = \sqrt{R_0^2 + L^2 - 2R_0L\cos\left[\psi + \arcsin(\frac{e}{R_0}\cdot\sin\varphi)\right]} \quad (32)$$

To simplify the obtained expression of the full driving force of the vibration exciter with a pendulum anti-skid device, the following transformations are performed:

$$tg\ arcsin(\frac{e}{R_0}\cdot sin\varphi)=\frac{\frac{e}{R_0}\cdot sin\varphi}{\sqrt{1-\frac{e^2}{R_0^2}\cdot sin^2\varphi}};\quad (33)$$

$$A=\sqrt{1-\frac{e^2}{R_0^2}\cdot sin^2\varphi};\ \text{or}\ A=\sqrt{1-K_e^{-2}\cdot sin^2\varphi};\quad (34)$$

$$A_1=\sqrt{1-\frac{e^2}{R_{01}^2}\cdot sin^2\varphi_1}\ \text{or}\ A_1=\sqrt{1-K_{1e}^{-2}\cdot sin^2\varphi_1};\quad (35)$$

$$K_r=\frac{R}{L}=\frac{R_0}{L}\cdot(K_e^{-1}\cdot cos\varphi+A)=K_{0r}(K_e^{-1}\cdot cos\varphi+A);\quad (36)$$

$$\varphi_1=\varphi+arctg\frac{sin\psi}{K_{0r}\cdot(K_e^{-1}\cdot cos\varphi+A)-cos\psi}\quad (37)$$

After simplification, obtained in dimensionless form:

$$F_Y=\frac{P_y}{m\omega^2R_0}=(K_e^{-1}\cdot cos\varphi+A)\cdot\left[cos\varphi-\frac{2K_e^{-1}\cdot sin^2\varphi}{A}+\right.$$
$$\left.+K_M\cdot\sqrt{1+K_r^2-2K_r\cdot cos\psi}\cdot\left(cos\varphi_1-\frac{2K_{1e}^{-1}\cdot sin^2\varphi_1}{A_1}\right)\right]\quad (38)$$

where

$$K_{1e}=\frac{R_{01}}{e};\quad (39)$$

$$K_M=\frac{m_M}{m};\quad (40)$$

$$K_{0r}=\frac{R_0}{L};\quad (41)$$

In general, the dependence for the driving force PY has the form of a functional:

$$PY=m\omega 2R0\cdot f\left(\frac{m_M}{m};\frac{R_0}{e};\frac{R_0}{L};\varphi\right)\quad (42)$$

Graphs of the theoretical dependence of the specific force *Fy* from the carrier rotation angle φ, coefficient *Ke* and various mass of the pendulum anti-skid device are shown in fig. 5, 6, 7. The analysis of these graphs shows their significant asymmetry about the abscissa axis, and the asymmetrical shift of the driving force magnitude takes place in the direction of the eccentric displacement of the carrier rotation axis relative to the treadmill curvature center. With an increase in carrier eccentricity *e*, the graphs acquire a clearly defined saddle, limiting the maximum amplitude of the driving force [9].

The growth rate of *KM*, i.e. an increase in the load mass on the pendulum compared with the mass of the inertial slider provides an increase by a factor of 2-3 times the absolute value of the driving force and its momentum due to an increase in the total inertial moment of the planetary system.

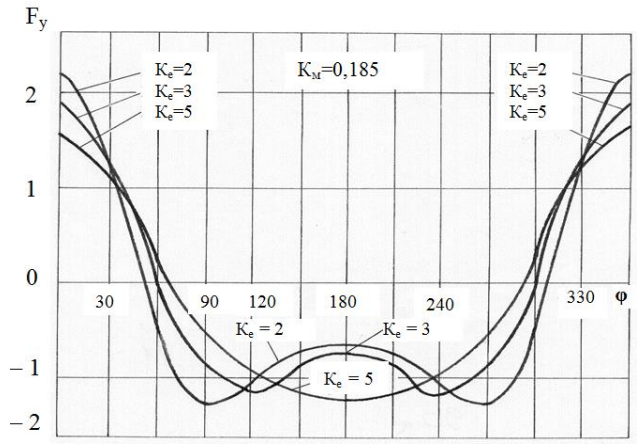

Figure 5. Dependence of the projection of the specific driving force of an asymmetric planetary exciter with pendulum anti-skid device on the ordinate axis from the carrier rotation angle

This indicates the feasibility of making part of the inertial mass of an asymmetric planetary vibroexciter in the form of a load mounted on the pendulum outside the treadmill in terms of the magnitude of the driving force.

A significant additional effect, provided by the pendulum device, is to force the slider against the treadmill surface and reduce the energy loss associated with the slider.

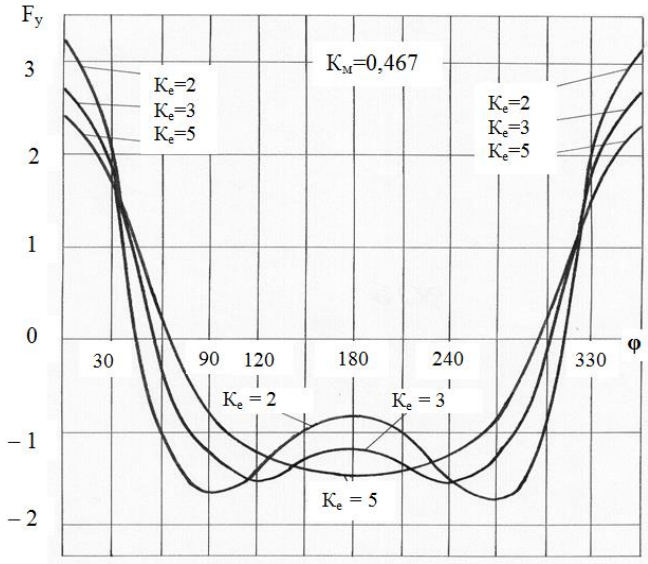

Figure 6. Dependence of the projection of the specific driving force of an asymmetric planetary exciter

with pendulum anti-skid device on the Y-axis from the carrier rotation angle at *KM = 0.467*

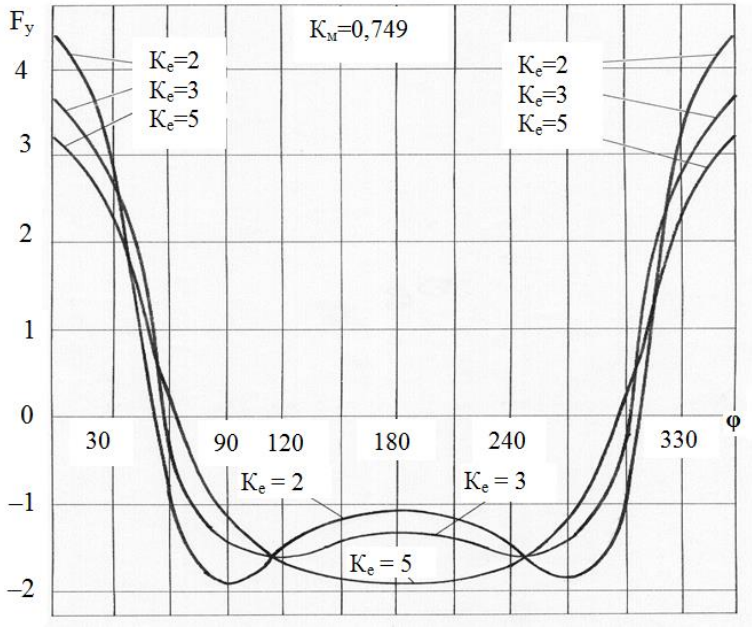

Figure 7. Theoretical dependence of the projection of the specific driving force of an asymmetric planetary vibration exciter with a pendulum anti-skid device on the ordinate axis from the carrier rotation angle at *KM* = 0.749

Conclusions. The theoretical analysis of the working process of a vibratory roller with an asymmetric planetary vibration exciter allows drawing the following conclusions:

1. Coriolis force acting on an asymmetric planetary vibration exciter provides a spontaneous torque of the slider causing slippage (skidding) of the slider on the treadmill, which is a negative factor leading to a sharp increase in energy intensity and heat density of the vibration exciter. The slip zones of the inertial slider along the treadmill surface of an asymmetric planetary exciter are determined from the condition of tangential forces equality acting at the point of slider contact with the treadmill and the traction forces of the slider with this track. The minimum value of the ratio of eccentricity to the treadmill radius, at which the slider slips, is K 0,196 (K =e/R0) at the points φ = 0 and φ = π of the motion path, and for skid at least K is slightly larger (0.35%) than for slider. Thus, the slider is a more dangerous critical mode of its movement compared to the skid.

2. The developed method for determining the critical inertial slider slip angles along the treadmill surface makes it possible to rationally select the design parameters of the planetary vibration exciter and additional means that prevent the inertial slider from slipping, which can provide a significant reduction in energy intensity of work, increase the efficiency and reliability of the vibration exciter.

3. Reducing the drive power and energy consumption of an asymmetric planetary vibroexciter, by preventing the inertial slider from slipping on the treadmill, can provide a mechanical anti-skid device in the form of a pendulum with an inertial mass (load) at the free end located outside the treadmill tracks.

4. For the first time, a theoretical model of an asymmetric planetary exciter with a pendulum anti-skid device, which adequately describes the dependence of the integrated driving force on

the initial parameters of the exciter, was obtained.

5. It has been established that an increase in the mass of the load on the pendulum compared to the mass of the inertial runner provides an increase in the absolute value of the driving force and its impulse by a factor of 2–3 due to an increase in the total inertial moment of the planetary system.

6. Invariance of the driving force of a planetary vibration exciter determines the possibility of its similarity in the geometric scale of modeling with the affine similarity of the inertial mass parameters, the angular velocity of the carrier, and the geometric parameters of the vibration exciter for the same structural schemes of the vibration exciter.

7. The different type of similarity criteria for the exciter and vibratory roller determines the different scales of modeling of these subsystems, and the linear scale of the exciter increases less intensively with increasing linear scale of the roller according to the law $K\ell = K\ell_в 2/3$.

Acknowledgments. This research has been funded by the Science Committee of the Ministry of Education and Science of the Republic of Kazakhstan (Grant No. AP09260192 Development of innovative milling-rotary snow-clearing working equipment with increased efficiency»).

References

1. Stryczek J., Banaś M., Krawczyk J., Marciniak L., Stryczek P. The Fluid Power Elements and Systems Made of Plastics, Procedia Engineering 176 (2017) 600-609.Published by Elsevier Ltd., www.elsevier.com/locate/procedia.
2. Giel, R., Młyńczak, M., Plewa, M. Evaluation method of the waste processing system operation. Risk, Reliability and Safety: Innovating Theory and Practice - Proceedings of the 26th European Safety and Reliability Conference, ESREL 2016.
3. Surashev N. et al., The Planetary Vibroexciter with Elliptic Inner Race, Advanced Materials Research, 2013:694-697:229-232, doi: 10.4028/www.scientific.net/AMR.694-697/229.
4. Doudkin M.V., Pichugin S.Yu., Fadeev S.N. The Analysis of Road Machine Working Elements Parameters // World Applied Sciences Journal. 2013. Vol. 23. Issue 2. P. 151-158. (ISSN / E-ISSN: 1818-4952/1991-6426). IDOSI Publications, 2013.DOI: 10.5829/idosi.wasj.2013.23.02. 13061.
5. ErmilovA.B. Teoreticheskij analiz raboty asimmetrichnogo planetarnogo vibrovozbuditelya s mayatnikovym ustrojstvom protivoskol'zheniya. Deponirovana VCNIITEH strojmash, № 24 – p. 91.– M.: MADI, 1991. – 11 p.
6. S.U. Dzholdasbekov, Y.S.Temirbekov. Shock-free Race Track of Road Roller Vibration. Exciters Proceedings of the World Congress on Engineering 2011 Vol. III, WCE 2011, July 6 - 8, 2011, London, U.K.
7. Fedotov, A.I., Młyńczak, M. Simulation and experimental analysis of quality control of vehicle brake systems using flat plate tester. Advances in Intelligent Systems and Computing. 2016.
8. Bostanov B.O. Razrabotka kinematiki i dinamiki kombinirovannogo vibrovozbuditelya dorozhnyh katkov: dis. … kand. tekhn. nauk: 05.05.04/ B.O. Bostanov. – Almaty, KazNTU, 2010. – 172 p.
9. Doudkin M.V., Vavilov A.V., Pichugin S.Yu., Fadeev S.N. Calculation of the Interaction of Working Body of RoadMachine with the Surface. Life Science Journal. 2013. Vol. 10. Issue 12. Article number 133:832-837.doi:10.7537/marslsj1012s13.133.
10. Pichugin S.Yu.et al. Studying the Machines for Road Maintenance // Life Science Journal.2013. Vol. 10. Issue 12. Article number 24- P. 134-138. doi:10.7537/marslsj1012s13.24.
11. Fadeev S.N., Pichugin S.Yu., Doudkin M.V. Contact Force Calculation of the Machine Operational Point // LifeScience Journal. 2013. Vol. 10. Issue 10. Article number 39-P. 246-250. (ISSN: 1097-8135). doi:10.7537/marslsj140817.39,http://www.lifesciencesite.com. 39.
12. Kim A., Doudkin M., Vavilov A., Guriyanov G. New vibroscreen with additional feed elements, Archives of Civil andMechanical Engineering 17 (4) 2017:786-794 http://doi.org/10.1016/j.acme. 2017.02.009.
13. M. A. Sakimov, A. K. Ozhikenova, B. M.Abdeyev, M. V. Dudkin, A. K. Ozhiken, S. Azamatkyzy.

Finding allowable deformation of the Road Roller Shell with variable curvature. News of the National Academy of Sciences of the Republic of Kazakhstan, Series of Geology and Technical Sciences. issn 2224-5278. Volume 3, Number 429 (2018), 197 – 207.
14. R. Gabdyssalyk, Y. I. Lopukhov, M. V. Dudkin. Study of the structure and properties of the metal of 10Cr17Ni8Si5Mn2Tigrade during cladding in a protective atmosphere. News of the National Academy of Sciences of the Republic of Kazakhstan, Series of Geology and Technical Sciences. issn 2224-5278. Volume 2, Number 428 (2018), 95-103.
15. Ermilov A.B., Doudkin M.V. Opredelenie granichnyih usloviy proskalzyivaniya inertsionnogo begunka asimmetrichnogo planetarnogo vibrovozbuditelya. – M.: MADI, 1988. – 9s. – Dep. V TsNIITEstroymash, 86 – 88.
16. Ermilov A.B., Doudkin M.V. Opredelenie granichnyih usloviy proskalzyivaniya inertsionnogo begunka asimmetrichnogo planetarnogo vibrovozbuditelya. – M.: MADI, 1988. – 9s. – Dep. V TsNIITEstroymash, #86-88.
17. E. S. Temirbekov, B. O. Bostanov, M. V. Dudkin, S. T. Kaimov and A. T. Kaimov. Combined Trajectory of Continuous Curvature. Advances in Italian Mechanism Science. Proceedings of the Second International Conference of IFToMM Italy. Mechanisms and Machine Science (MMS 68). Volume 68. IFToMM ITALY, pp. 12–19, 2019. Springer Nature Switzerland AG, 2019. ISBN 978-3-030-03319-4. https://doi.org/10.1007/978-3-030-03320-0_2
18. M. Doudkin, A. Kim, V. Kim, M. Mlynczak, G. Kustarev. Computer Modeling Application for Analysis of Stress-strain State of Vibroscreen Feed Elements by Finite Elements Method. Mathematical Modeling of Technological Processes International Conference, CITech 2018, Ust-Kamenogorsk, Kazakhstan. September 25-28, 2018 Proceedings. – P.82-96. https://doi.org/10.1007/978-3-030-12203-4_9
19. B. O. Bostanov, E. S. Temirbekov, M. V. Dudkin, A. I. Kim. Mechanics-Mathematical Model of Conjugation of a Part of a Trajectory with Conditions of Continuity, Touch and Smoothness. Mathematical Modeling of Technological Processes International Conference, CITech 2018, Ust-Kamenogorsk, Kazakhstan. September 25-28, 2018. Proceedings. – P.71-81. https://doi.org/10.1007/978-3-030-12203-4_8
20. Mikhail Doudkin, Alina Kim, Vadim Kim. Application of FEM Method for Modeling and Strength Analysis of FEED Elements of Vibroscreen. Proceedings of the 14th International Scientific Conference on Computer Aided Engineering, June 2018. Series: Lecture Notes in Mechanical Engineering. - Wrocaw, Poland, - 2019, 892 p.